中國機械工程學刊第四十二卷第五期第 501~507 頁(民國一百一十年)
Journal of the Chinese Society of Mechanical Engineers, Vol.42, No.5, pp. 501~507 (2021)

Contact Force Experiments and Deformation Analyses of a Cobra Needle Used in Vertical Wafer Probe Card

Jinn-Tong Chiu* and Dar-Yuan Chang**

Keywords：Wafer testing, Vertical wafer probe card, Contact force, Image processing, Finite element analysis.

ABSTRACT

Wafer testing requires a probe card with a mass of microprobes as a contact medium between the prober and the wafer. Electric characteristics of the examined welding pads are tested by direct contacts between the microprobes and pads. These needles are subject to deflection or buckling resulting from the contact test, and might lose their original strength. To understand the loading state and deformation process of the needle, this study develops a microprobe testing platform for analyzing a vertical cobra needle. Testing parameters which affect the contact force were investigated, such as the probing overdrive, approaching speed, and probing time. Needle deformation during probing was observed by a computer vision system and evaluated by image processing methods. Furthermore, the finite element model of a palladium alloy cobra needle was established to simulate its contact behaviors in wafer probing for obtaining a wafer probe card with correct test and robust performance.

INTRODUCTION

Probe card is a key instrument in wafer testing which serves as a contact medium between the prober and the wafer, as shows in Fig. 1. A large number of microprobes which laid according to the welding pads are fixed on the probe card. The microprobes form a high density acicular surface and make direct touch with the examined pads to be tested individually. An accurate positioning probe card allows correct electric connections between the needles and examined pads, and hence measures electrical functionalities of the wafer dies. The fabrication level of the probe card significantly affects the correctness of wafer testing. At present, a vertical probe card is commonly used to test the IC product with array pads. Fig. 2 shows a schematic diagram of the vertical probe card with a cobra needle.

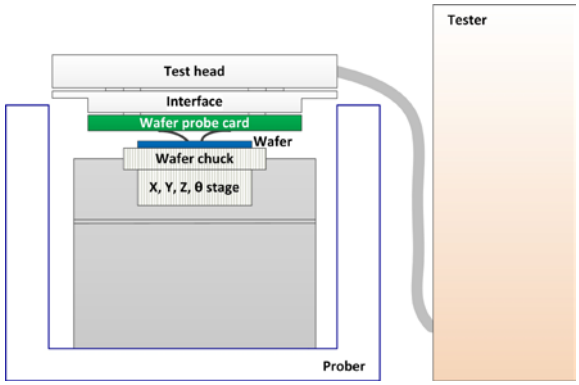

Fig. 1. Wafer testing system.

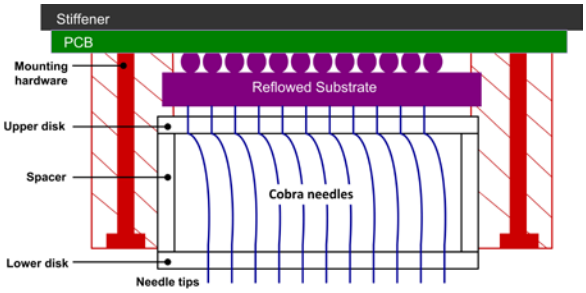

Fig. 2. Structure of a vertical probe card with cobra needles.

A probing overdrive (OD) is the probe card displacement in the probing direction after the needles touch the examined wafer. It ranges from 25 to 100 μm (1 to 4 mil) commonly. A suitable overdrive results in an appropriate probing force on the surface of the welding pad so that the surface oxide film is then broken by a scrub motion and gets

Paper Received January, 2015. Revised March, 2016, Accepted December, 2016, Author for Correspondence: Jinn-Tong Chiu.

* *Professor, Department of Systems Engineering and Naval Architecture, National Taiwan Ocean University. Keelung, Taiwan 202301, ROC.*

** *Professor, Department of Mechanical Engineering, Chinese Culture University. Taipei, Taiwan 11114, ROC.*

the objective of electric conductions. Factors affecting the length of scrub mark include the shape and diameter of the needle tip, contact force on the needle tip, coplanarity of the acicular needle tips, and material of the welding pad. An insufficient overdrive results in a poor connection, while an excessive overdrive would damage the welding pad and increase the wear on the needle tips, shortening its working life.

Four characteristics of the contact resistance, contact force, alignment accuracy, and length of scrub marks, require testing in probe card fabrication. Factors affecting the contact resistance include materials of the pad and needle, needle geometry, contact force on the needle tip, and so on. Borz and Rincon (1999) introduced a contact theory for interaction between the needle tip and the pad. They revealed the effect of temperature rise on probe contact resistance in wafer testing. Experimental results for an aluminum pad show that contact resistance increases rapidly for tungsten (W) and tungsten-rhenium (WRe) needles under a high probing temperature. Beryllium copper (BeCu) needles exhibit more stable behaviors in comparison. There is less accumulated debris for WRe needles, and therefore the contact resistance appears to be more stable. Liu et al. (2007) measured the contact resistance to quantify the level of contamination on the needle tip caused by accumulated particles and to determine whether needle's function is normal. The contact resistance between the tungsten needle and copper foil is 100 mΩ. The measured resistance becomes stable at an overdrive of 45 μm After 30,000 contacts, the contact resistance exceeds 1 Ω. Therefore, the needle must be removed for cleaning to maintain a contact resistance less than 1 Ω.

The force applied on the examined pad by the probing needle during wafer testing is called the contact force. Contact force and overdrive have a positive correlation. The general design rule is to induce a contact force ranged from 2 to 5 g under an overdrive of 0.001 inch for a single needle, that is, 2-5 g/mil/pin. However, the contact force and resistance are in a reciprocal relation. When the needle penetrates the surface oxide film of the welding pad, contact resistance decreases rapidly as the contact force increases. Excessive overdrive may damage the welding pad while insufficient overdrive cannot break the oxide film and may result in a poor connection. Comeau and Naduau (1991) developed a mathematical model for deducing the effects of overdrive on contact force and displacement. Maekawa et al. (2000) discussed the relationships between the shape of needle tip and the plastic deformation on the aluminum pad for a cantilever probe card. In addition, the influence of the roughness of needle tip on the aluminum adhesion was also revealed. Liu and Shih (2006) presented a wafer testing parameter study for cantilever type probe cards. They employed experimental and numerical methods to investigate the correlations between the overdrive, contact force, and scrub mark length. Probe displacement is defined as the distance between the centers of needle tip and the welding pad or that between the scrub mark and the examined pad at the end of probing stroke. It can be used to represent the alignment accuracy. Chang and Choi (2009) developed a finite element model for a cantilever type needle. Taguchi's method was employed to analyze the contact force and displacement on the needle tip. A series of sensitivity experiments were performed to optimize the probe geometry.

Considering the difficulty in directly measuring the coplanarity on an acicular surface formed by the needle tips, the scrub mark on the examined pads have become an important assessment characteristic to show the fabricating level of probe cards. A long scrub mark is made by a lower needle. A deep scrub mark indicates more materials are accumulated at the end of the mark, the needle tip sustains a large contact force, and more wear is produced on the needle tip leading to a short working life. Irregular distribution of scrub marks of varying depth indicates a poor coplanarity. Chang, et al. (2013) presented a method to simulate the bump wafer probing. Three-dimensional finite element models were built and validated by experiments for the bump height variation and scrub mark area on the solder bump influence.

Most studies address the contact issues of the cantilever probe card, and research on the vertical probe card is scarce. This study focuses on the problems of the vertical probe card. A microprobe testing platform for a vertical cobra needle was constructed to investigate the influences of wafer testing parameters on the contact force at the needle tip. A high-speed camera and image processing methods were used to record and measure the deformation of the needle body in the contact experiments. In addition, a finite element model of the cobra needle was established for providing more detailed observations in the contact behaviors.

MICROPROBE TESTING PLATFORM

The Vertical Cobra Needle

Hauck et al. (2010) presented a nonlinear buckling analysis on the vertical wafer probes. The critical load according to Euler's formula is:

$$F_c = \frac{\pi^2 EI}{(K_i l)^2}, \tag{1}$$

where E is Young's modulus, I is the moment of inertia, l is the length, and K_i is the effective-length factor. Problems can be divided into four types based on the boundary conditions: (1) One end is fixed, and the other end is free, K_i= 2; (2) Both ends are pinned,

K_i= 1; (3) One end is fixed, and the other end is pinned, K_i= 0.699156; and (4) Both ends are fixed, K_i= 0.5.

The cobra needle was patented by Byrnes and Wahl (1997), which has been widely used in vertical probe cards as shown in Fig. 3(a). Both ends of the needle have a circular cross section while the cross section of the needle body that stores energy is rectangular. Figure 3(b) is a picture of the cobra needle, 4 mil in diameter, at 10 times magnification. To give an indication of scale, the black circle has a diameter of 1 mm. The loading state of the vertical needle belongs to the third category, i.e., one fixed end and one pinned end. Chiu and Chang (2009) proposed a cobra needle design approach for reducing the maximum stress used in vertical probe card. The method combines the nonlinear finite element method with the quadratic searching optimization to derive the optimal geometry design of the cobra body.

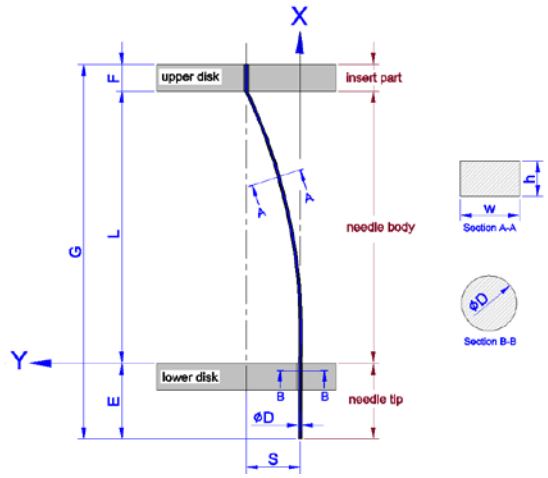

(a)

(b)

Fig. 3. The cobra needle: (a) structural drawing and (b) actual object.

Testing Platform

This study develops a microprobe testing platform that consists of a micro-stage, computer vision system, probe clamming apparatus, and load cell module, as Fig. 4 shows. Table 1 lists the main components of the system. The vertical axis of the micro-stage is driven by a high-precision stepping motor, and controlled by the LabVIEW software. It offers a control accuracy of 0.001 mm which provides sufficient orientation for simulating the OD in wafer probing.

To observe the deformation process of microprobes during probing, a computer vision system is mounted at the direction normal to that of the probing. Contact behaviors of the examined needle are recorded using dynamic imaging techniques. The imaging system that includes a high-speed color camera with 2X zoom connected to a 70X C-mount microscopic lens, a 3200 W halogen light (FO-150H), and the StreamPix5 software under the Windows 7 operating system. The highest resolution is 659×494 pixels and 196 photos can be captured per second. The lowest resolution is 40×40 pixels and 1691 photos can be obtained at most. Geometric variation of the needle is further analyzed through digital image processing methods.

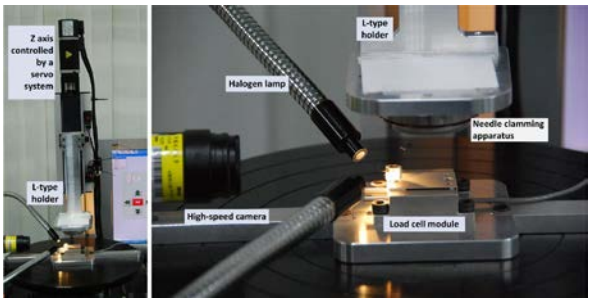

Fig. 4. Microprobe testing platform.

Table 1. Components of the testing platform.

Devices	Components
Driver	Motor: PK545NAW, DC24V, fundamental stepping angle 0.72°. Controller : EMP402 (ORIENTAL MOTOR)
Images apparatuses	High-speed camera: PicSight G32B-GigE; C-mount microscopic lens: VSZ0745, 70X; Halogen light: FO-150H; Software: StreamPix5. Maximum resolution 659×494 pixels.
Load cell	GMI SBC-250, HSM display; Precision: 0.125 grams.

Needle Clamming Apparatus

The probe clamming apparatus is a five-layer design fixed below the L-shaped holder, as shown in Fig. 5. From the top, there are jig, substrate (ST), upper disk (UD), spacer, and lower disk (LD). The examined needle is placed through the UD, spacer, and LD. The combination of UD, spacer, and LD is called a probe head. To fit the image capturing system, the apparatus has a side opening. As many as nine needles can be mounted on the device in the opening region. A load cell module is placed under the needles, as Fig. 4 shows. A welding pad stand made of isolating ABS is mounted on the load cell detecting shaft. A load cell of GMI SBC-250 with HSM monitor is employed in this study. Its recording speed (response frequency) is 20 Hz.

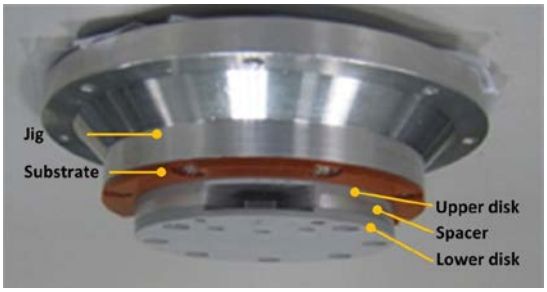

Fig. 5. Probe clamming apparatus.

FINITE ELEMENT MODEL

A nonlinear finite element model of the cobra needle is constructed to perform the stress and deformation simulations. Linear material and nonlinear geometry are considered in modeling. The finite element model is described as follows.

Governing equations

Based on the theory of large deformation, a finite element model is constructed based on a total Lagrangian approach. The equilibrium equation can be expressed under virtual work principle as (MARC 2020):

$$\int_{V_0} S_{ij}\delta E_{ij}dV = \int_{V_0} b_i^0 \delta\eta_i dV + \int_{A_0} t_i^0 \delta\eta_i dA, \quad (2)$$

where S_{ij} is the symmetric 2nd Piola-Kirchhoff stress tensor; E_{ij} is the Green-Lagrange strain tensor; b_i^0 is the body force vector corresponding to the reference coordinate system; t_i^0 is the applied force vector corresponding to the reference coordinate; and η_i is the virtual displacement. Integrating from t = 0, the strain is expressed as the sum of total strain of equilibrium and incremental strains accumulated, from t = n to t = n+1.

Von Mises stresses are adopted as the stress criterion, and can be written as:

$$\bar{\sigma} = [(\sigma_x-\sigma_y)^2+(\sigma_y-\sigma_z)^2+(\sigma_z-\sigma_x)^2+6(\tau_{xy}^2+\tau_{yz}^2+\tau_{xz}^2)]^{1/2}/\sqrt{2}. \quad (3)$$

Simulations of a Palladium Alloy Cobra Needle

A cobra needle consists of an insert part, needle body, and needle tip as shown in Fig. 3. The needle body is formed from a circular section into a rectangle and bended to the expected curvature by the presswork. The bending needle body provides energy and elasticity required in wafer probing. A palladium alloy cobra needle with a 4-mil diameter was analyzed here. The needle geometry is shown as Fig. 3(a). Dimensions of the needle are given in Table 2.

Table 2. Dimensions of the simulated needle.

Dimensions	S	L	D	E	F	G	w	h
Measured data (mm)	1.219	3.683	0.102	2.159	0.635	6.477	0.1398	0.058

A dynamic transient analysis is used to simulate the needle probing process. The finite element model of the simulated needle was established by the FEM software MARC, which has 17280 solid elements and 19783 nodes. The needle is assumed as an elastic material with a Young's modulus of 97 GPa and a Poisson's ratio of 0.284. The boundary at the end of the insert part is fixed. The interface between the needle tip and lower disk is considered as a contact boundary, as well as for that between the contact surface of the needle tip and welding pad. The Coulomb stick-slip friction model is used to simulate the friction of contact surface. The friction coefficient of each contact surface is 0.1. Elastic deformation of the lower disk and welding pad is ignored and they are modeled as a rigid surface. A relative displacement (overdrive) of 100 μm between the probe and welding pad was introduced in order to simulate mechanical behaviors of the probe during wafer testing. The total probing time is 8 secs, and from 0 to 1 sec welding pad is closing to needle tip by uniform velocity, and from 1 to 5 sec the welding pad is stop with 100 μm overdrive, and from 5 to 6 sec the welding pad is removing from the needle tip by uniform velocity.

Fig. 6 shows the contact force simulated and the OD track which imitated the motion of testing platform. The maximum contact force is 16.8 g. The probe temperature rises about 4 °C when the applied test voltage is 0.4 V. Therefore, the stiffness and strength variations from temperature raised are neglected. The von Mises stress distribution simulated is shown as Fig. 7. The maximum von Mises stress of 802 MPa occurs at the end of insert part, which is less than the yield stress of 1103 MPa provided by the microprobe supplier (Acme Technology Inc.). The maximum lateral displacement was 0.186 mm occurred at the middle of the bending body.

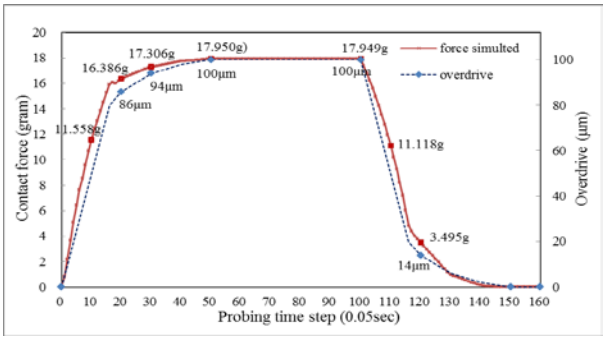

Fig. 6. The contact forces simulated and the OD track in FE simulations.

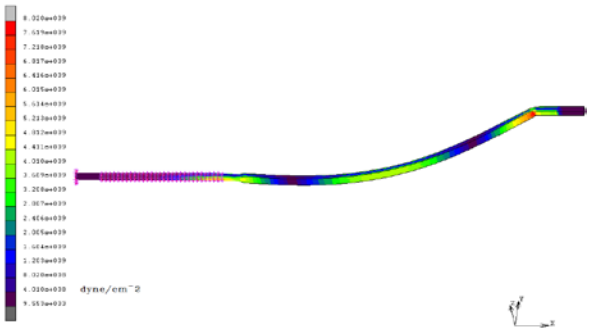

Fig. 7. Distribution of the von Mises stress under an OD of 100 μm.

COBRA NEEDEL PROBING EXPERIMENTS

Experimental Plan

In wafer testing, the wafer is moved up (with the chuck) to contact with the group of needles, and needles' body are deformed and absorbed energy like a micro-spring. Testing parameters of the probing overdrive, approaching speed, and probing time were investigated in this study. Seven different OD are experimented from 25 μm to 175 μm with an interval of 25 μm (1 mil).

Needle deformation analyses

From the structure of the cobra needle, the needle body is designed for energy absorption acting as a micro-spring. According to the simulation results in previous section, the maximum deformation occurs at the middle of the needle body. Fig. 8 shows a series of probe images extracted from the dynamic pictures. These images were further processed by the image tools in MATLAB, and the needle deformation process can then have a clear inspection.

Digital data of the images representing the needle's shape are obtained after the treatments of grayscale treatment, binary treatment, and skeletonization, as shown in Fig. 9. From the skeletonized image, the bending area can be calculated. In this case, 1 pixel represents an area of 0.001156 mm^2. The bending area of the needle body can be obtained by counting the number of pixels covered in the region between UD and LD, as the region 'A' shown in Fig. 9(e).

Experimental Results and Discussion

(1) *Probing overdrive.* The contact force and bending area of the needle body were measured from under different ODs. Approaching speed was specified as a constant of 10 mm/s and the probing time was 2000 ms. Measurement was taken at an OD increment of 25 μm (1 mil). Experimental results are presented in Fig. 10. Both contact force and bending area are increased as the increase of OD. The contact force on the needle tip exhibits a linear increase with a gradient of 4.8 g/mil. The contact force for the 4 mil OD which mostly used is 19.15 g/mil. The following are two characteristic polynomial equations regressed:

$$F_{contact} = -0.0882x^3 + 1.0007x^2 + 1.6348x + 2.2878, \quad (4)$$

$$Area_{bend} = -0.0069x^2 + 0.128x + 2.93, \quad (5)$$

where x is the OD in μm. Understanding the probing characteristics enables engineers to determine a suitable OD for providing sufficient contact force in wafer testing.

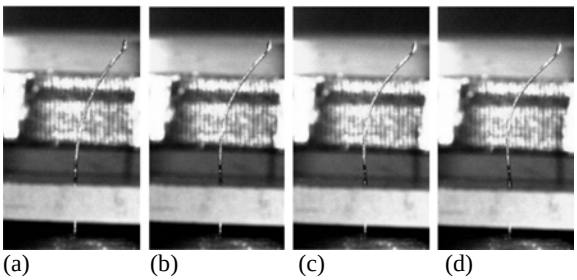

(a) (b) (c) (d)

Fig. 8. Images of the needle deformation process captured under different OD: (a) 25 μm (b) 75 μm (c) 125 μm (d) 175 μm.

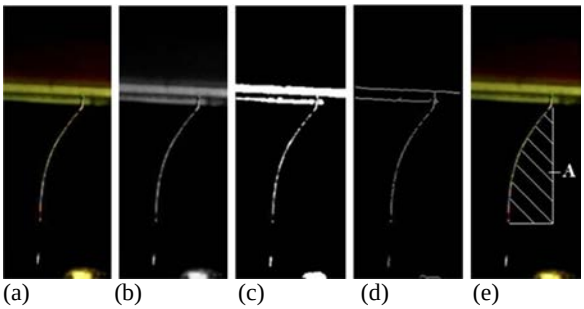

(a) (b) (c) (d) (e)

Fig. 9. Images of the image processing treatments: (a) original, (b) grayscale, (c) binary, (d) skeletonized, and (e) bending area calculation.

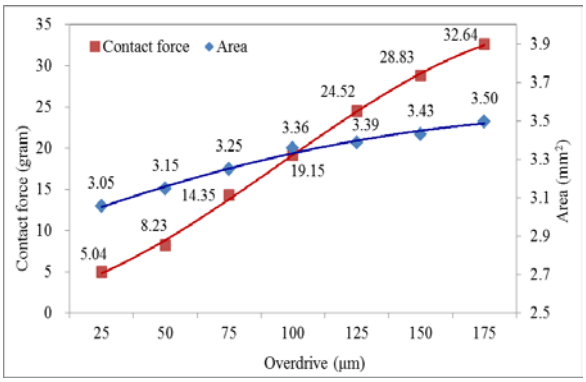

Fig. 10. Contact force and needle bending area of the probing overdrive experiments.

(2) *Approaching speed.* A high needle approaching speed can reduce the testing time, thus lower the cost. The Z-axis linear speed of the micro-stage in this study could be controlled in a precision of 0.01 mm/s.

Seven approaching speeds were experimented from 10 to 130 mm/s with an interval of 20 mm/s, and the OD and probing time were fixed at 100 μm and 2000 ms, respectively. Figure 11 shows the experimental results. Within the test range, a slight linear decrease is observed in both the contact force and bending area. It is worth noticing that increasing the approaching speed from 30 mm/s to 130 mm/s leads to approximately 1 gram reduction in the contact force.

(3) ***Probing time.*** After the needle comes into touch with the examined pad, it enters a metastable state before reaching a stable probing force. In this study, 95% of the maximum contact force was set as a critical probing force, beyond which point a stable state is assumed. Figure 12 shows a case with a probing time of 5 seconds. The OD is set at 100 μm and the approaching speed is 10 mm/s. The maximum contact force of 17.65 grams is reached (marked by the blue point) at the time of 3.05 seconds (the 61st time frame). The critical probing force is therefore 16.77 grams based on the definition of 95% maximum force. At the 1.3 seconds (the 26th time frame), the contact force increases to 16.8 grams (marked by the red point). Consequently, the probing time in this case should be more than 1.3 seconds. Comparing with the simulating results in Fig. 6, both the FE simulation and actual experiment have coincident results. The simulation model developed in this study has been proofed.

The time to reach the critical probing force varies with different ODs. The relationships between the contact force and probing time for the seven experiments are presented in Fig. 13. Results show that for a small OD, the time required to reach the critical probing force is longer than a large OD; however, the time to reach the maximum probing force is relatively short. When the testing is in a large OD, it takes a long time to provide the forces from the critical to the maximum.

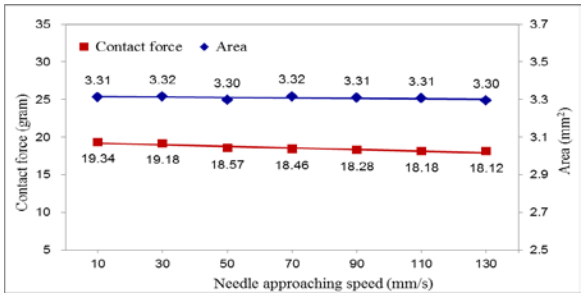

Fig. 11. Contact force and needle bending area of the approaching speed experiments.

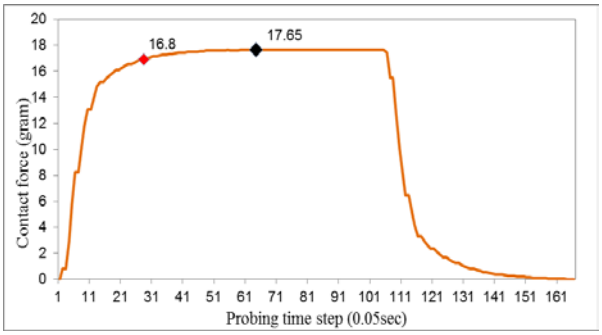

Fig. 12. Relationship between the contact force and probing time.

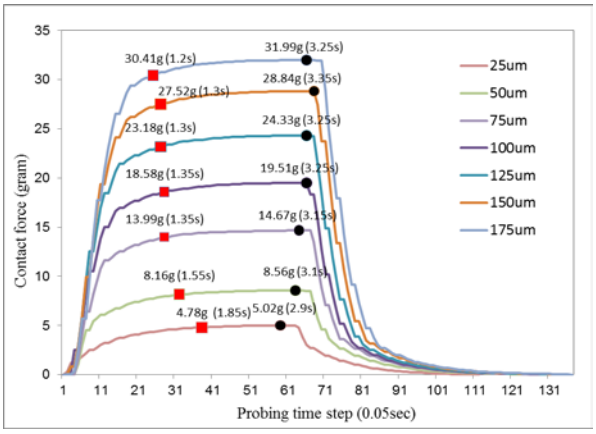

Fig. 13. Critical and maximum contact forces in different ODs.

CONCLUSIONS

A microprobe testing platform for the cobra needle was developed in this study to measure the contact force on the needle tip and to observe the deformation of the needle body in wafer probing. This platform is an integration of a micro-stage, needle clamming apparatus, computer vision system, and load cell module. From the results of the Cobra needle probing experiments, two regressive equations of the overdrive to the contact force of the microprobe and bending area of needle body were derived. Although the approaching speed does not have much impact on the contact force, the probe must pass a period of metastable state before it reaches the stable contact force. The duration of this state depends on the OD. Results of finite element simulations show that the maximum von Mises stress occurs at the end of the insert part and the maximum displacement is near the middle of the needle body. This paper presents valuable data on contact force and needle deformation of a palladium alloy Cobra needle used in the vertical wafer probe card.

ACKNOWLEDGEMENT

Financial support for this work was provided by the National Science Council Taiwan, R.O.C, under the contract NSC-100-2221-E-034-002.

REFERENCES

Bronz J.J. and Rincon R.M., "Probe Contact Resistance Variations during Elevated Temperature Wafer Test," *IEEE International Test Conference* 1999, Paper 15.3, pp.396-405 (1999).

Byrnes H.P. and Wahl R., "Contact for an electrical contactor assembly," *United States Patent* 4027935, 1977.

Chang D.Y. and Choi J.T., "Geometric Parameter Design of a Cantilever Probing Needle used in Epoxy Ring Probe Card," *Journal of Material Processing Technology*, Vol. 209, pp. 38-50 (2009).

Chang H.Y., Chang K.H., Lai Y.S., "Experimental Testing and Finite Element Modeling of Bump Wafer Probing," *Applied Mechanics and Materials*, Vol. 284-287, pp. 748-753 (2013).

Chiu J.T. and Chang D.Y., "A new probe design combining finite element method and optimization used for vertical probe card in wafer probing," *Precision Engineering*, Vol. 33(4), pp. 395-401 (2009).

Comeau A.R. and Naduau N., "Modeling the bending of probes used in semiconductor industry," *IEEE Transactions on semiconductor manufacturing*, Vol. 4(2), pp. 122-127 (1991).

Hauck T., Muller W.H. and Schmadlak I., "Nonlinear buckling analysis of vertical wafer probe technology," *Microsystem Technology*, Vol. 16, pp. 1909-1920 (2010).

Liu D.S. and Shih M.K., "Experimental method and FE simulation model for evaluation of wafer probing parameters," *Microelectronics Journal*, Vol. 37, pp. 871-883 (2006).

Liu D.S., Shih M.K. and Huang W.H., "Measurement and analysis of contact resistance in wafer probe testing," *Microelectronics Reliability*, Vol. 47, pp. 1086-1094 (2007).

Maekawa S., Takemoto M., Kashiba Y, Deguchi Y., Miki K. and Nagata T., "Highly reliable probe card for wafer testing," 2000 Proceedings. 50th Electronic Components and Technology Conference, pp. 1152-1156 (2000).

MARC Volume A: Theory and User Information, Version 2020, MARC Analysis Research Corporation, 2020.

垂直式晶圓探針卡之探針接觸力實驗與變形分析

邱進東
國立台海洋大學 系統工程暨造船學系

張達元
中國文化大學 機械工程系

摘 要

晶圓測試需要藉探針卡上的大量微探針做為接觸介質，透過微探針和晶圓焊墊間的直接接觸，檢驗受測焊墊的電子特性。這些探針會因接觸測試所發生的撓曲或屈曲現象，而失去其原始強度。為了了解針的加載狀態和變形過程，本研究開發了適用於分析垂直式 Cobra 探針的微探針測試平台，分析影響探針接觸力的測試參，包括：針測行程、針測速度、以及測試時間。針測過程中的探針變形由電腦視覺系統觀察並配合數位影像處理方法進行評估。此外，本文建立了鈀合金 Cobra 探針的有限元素模型，模擬微探針於晶圓針測行程中的接觸行為，以獲得具有正確測試功能與穩健性的晶圓探針卡。